ChemComm

ROYAL SOCIETY
OF CHEMISTRY

COMMUNICATION

View Article Online
View Journal

Check for updates

Cite this: DOI: 10.1039/d1cc00453k

Received 26th January 2021,
Accepted 14th April 2021

DOI: 10.1039/d1cc00453k

rsc.li/chemcomm

Synthesis of hydrogen-substituted graphdiynes *via* dehalogenative homocoupling reactions†

Jiasheng Wu, Jizhe Liang, Yijie Zhang, Xiaoli Zhao* and Chunxue Yuan *

A new method is introduced to prepare hydrogen-substituted graphdiynes (HsGDYs) *via* the dehalogenative homocoupling of terminal alkynyl bromides. Compared with previous synthetic strategies, the reaction conditions are moderate and the time is shortened. HsGDYs exhibit porous structures and hydrogen/oxygen evolution reaction (HER/OER) catalytic activity, endowing applications in electrochemical catalysis.

Graphdiyne and its analogues (GDYs), as a rising star of the carbon family, are a series of artificial two-dimensional nanomaterials which contain sp and sp^2 hybridized carbon atoms. Different from graphene, the introduction of alkynyl bonds renders GDYs unique physical and chemical properties. This extended π-conjugated system endows GDYs with a natural band gap of 0.44 to 1.47 eV and a high carrier mobility of 10^4 to 10^5 $cm^2\ V^{-1}\ s^{-1}$.[1] GDYs consist of aromatic rings connected with diacetylenic bonds, dictating a flat structure with evenly dispersed pores. Combining the uniform nanoscale porosity and exceptional electronic properties, GDYs show great potential in the fields of energy storage, catalysis, sewage treatment, *etc.*[2–8] More than that, by altering precursors, the pore size can be precisely controlled and GDYs with different heteroatoms (such as Cl, F, N, and H) can be obtained.[3,4,6,9–14] Compared with GDY, HsGDY has lower atom density and larger pore size which facilitate ion diffusion parallel and perpendicular to the basal plane. The vicinity of these extra hydrogen atoms also leads to the promotion of ion storage capacity.

Though Baughman predicted the existence of graphyne in 1987, the preparation remained a challenge until Li and co-workers' ground-breaking work in 2010.[15,16] So far, the synthetic strategies for GDYs have been classified into wet chemistry and dry chemistry. For wet chemistry approaches, the reactions related can be divided into two types according to the functional groups.[17] The first type is the homocoupling reaction of monomers with terminal alkynyl groups. Among them, Glaser, Glaser–Hay and Eglinton coupling reactions are the most commonly utilized.[4,16,18–23] However, due to the high reactivity, such monomers face the risk of oxidative deterioration during the whole process and extra heating is usually required. The homocoupling of terminal alkynylsilane groups is the other type. As a protection group, trimethylsilyl can significantly enhance the stability and directly yield the coupling products without deprotection (like Hiyama coupling).[24,25] However, for the preparation of GDYs *via* the homocoupling reaction of hexakis[(trimethylsilyl)ethynyl]benzene, the efficiency is low and various byproducts are generated.[17,24] Thus, exploiting new precursors with both great stability and high reactivity is highly desirable.

Beyond wet chemistry, dry chemistry is another powerful approach, such as the explosion approach and chemical vapor deposition.[26,27] We recently designed **tBEP** and successfully constructed two-dimensional molecular networks with acetylenic scaffoldings on Au(111) under ultrahigh vacuum.[28] During the synthesis process, the terminal alkynyl bromides of **tBEP** revealed higher stability than terminal alkynyl and dehalogenative C–C coupling yielded higher selectivity and fewer byproducts than the dehydrogenative ones. Naturally, this interesting phenomenon raised our curiosity about the possibility of constructing HsGDYs with terminal alkyne bromides *via* the dehalogenative homocoupling reaction in the solution phase.

Herein, we successfully prepared HsGDY films in solution *via* the dehalogenative homocoupling reaction of terminal alkynyl bromide molecules. HsGDY is a free-standing film with continuous large area not only from the view of the macroscopic morphology but also well-organized gauze-like membrane structures in the micronic scale. HsGDY consists of aromatic rings connected with a conjugated diyne linkage, as confirmed by a series of measurements. Besides, HsGDY shows an electrochemical catalytic performance comparable with previous reports.[7,29] Our strategy is substantially efficient and facile compared with previous ones, demonstrated by the shortened reaction time and room temperature conditions. This work proposed a novel path for the

---

College of Materials Science and Engineering, Tongji University, Shanghai, 201804, China. E-mail: cxyuan@tongji.edu.cn, zxl36@tongji.edu.cn

† Electronic supplementary information (ESI) available: Experimental details and additional experimental results. See DOI: 10.1039/d1cc00453k

preparation of HsGDYs under mild solution conditions, reconstructing the fascinating result which could only be attained under severe ultrahigh vacuum conditions reported previously.

The synthetic routes of monomer **tBEP** and HsGDY are shown in Scheme S1 (ESI†). The detailed synthesis of **tBEP** was modified based on our previous work to shorten the reaction period and save costs without reducing the yield of **tBEP**.[28] Copper foils were washed and sonicated with 1 M HCl, acetone and ethanol for 15 min successively, dried under a flow of nitrogen, and used immediately. To a three-necked flask, the pre-treated copper foil and **tBEP** (10 mg) were added. Then the flask was sealed and filled with nitrogen. 10 mL pyridine was added into the flask and stirred for 2 minutes. After that, 1 mL NaOH aqueous solution (0.1 M) was added dropwise into the mixture. Without extra heating, the mixture was stirred under a nitrogen atmosphere at r.t. for 12 h. The copper foils were taken out and washed with acetone and ethanol in turn. A nearly transparent light-yellow film was obtained on the copper foils. We also conducted this reaction with (bromoethynyl)benzene and 3-(bromoethynyl)-1,1′-biphenyl and both reactions occurred smoothly under the same conditions with high yields (ESI†).

Through the dehalogenative homocoupling reaction of **tBEP**, the HsGDY film was successfully grown on copper foils in pyridine and NaOH aqueous solutions (Fig. 1a). The colour of the copper foils turns light yellow and the surface is no longer shiny after HsGDY growth. When removed from copper foils, this free-standing film is light yellow and nearly transparent with an area of 7 cm^2 (Fig. 1b). SEM was employed to observe the morphology details of the as-prepared HsGDY film. The thickness of this film is about 600 nm according to the cross-sectional SEM image (Fig. S6, ESI†). As shown in Fig. 2a, the surface of the sample contains abundant pores with different sizes. The pore diameter ranges from several micrometres to tens of nanometres. With further magnification, densely dispersed smaller pores of about several nanometres in diameter are observed (Fig. 2b). These open hierarchical pores give the HsGDY film a three-dimensional porous structure with high surface accessibility. For an efficient reaction and ion storage, this macro/mesoporous second-order structure provides abundant channels and vacancies.[11,12] Comparing the morphology of the bottom and the top surface, it can be found that the side close to the copper foil (Fig. 2b) is clearly flatter and more regular than the side away from the copper foil (Fig. 2c). In this reaction, the copper foil acts as not only the catalyst source but also the substrate for the formation of HsGDYs.[16] At the beginning, the surface of the copper foil is entirely exposed to the system and HsGDY forms and spreads over the surface along with the dehalogenative homocoupling of **tBEP**. As the reaction proceeds, the coverage of HsGDYs goes up and the proportion of the bare copper surface goes down. At some point, the formed HsGDYs would become the obstacle of the subsequent reaction and eventually cause the irregularity of the film.

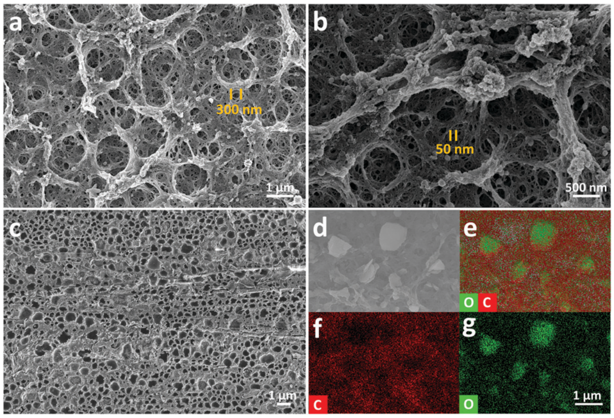

Fig. 2 SEM and EDS mapping images of HsGDY. (a, b) SEM images of the top side of a HsGDY film. (c) The SEM image of the bottom side of a HsGDY film. (d–g) EDS mapping images of C + O (e), C (f), and O (g) of HsGDY.

Since the structure of HsGDY can be regarded as replacing half of the acetylene bonds in GDY with hydrogen atoms, HsGDY theoretically possesses only two elements (carbon and hydrogen) and two kinds of hybridized carbon atoms (sp and sp^2).[30] Thus, an energy dispersive spectrometer (EDS) was employed to analyze the element composition of the sample. As depicted in Fig. 2e, the film is mainly composed of two elements: carbon and oxygen, mostly carbon. The oxygen is mainly concentrated on the external impurity particles (Fig. 2g) like the unreacted NaOH and the by-products, while the carbon spreads all over the film underneath in high density (Fig. 2f). The result of EDS proves the fact that the as-prepared HsGDY is a carbon-rich material. Fig. 3a shows the XRD patterns of the sample. The peak at 23.3° corresponds to an interlayer spacing of 3.81 Å. Due to the conformational fluctuation of HsGDY, the

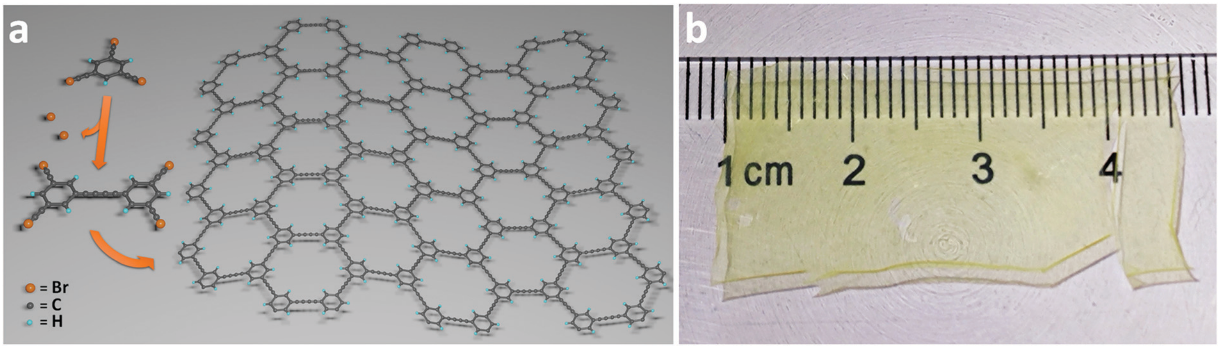

Fig. 1 (a) Schematic diagram of the dehalogenative homocoupling reaction and the chemical structure of HsGDY. (b) A photograph of the HsGDY film.

film we obtained is amorphous.[11,34] As depicted in Fig. 3b, the solid-state NMR of HsGDY indicates the existence of four types of carbon atoms. The peaks at 130.6, 123.5, 80.2, and 75.0 ppm correspond to aromatic C–C, aromatic C–H, C(sp)–C(sp^2) and C(sp)–C(sp), respectively.[11]

In characterizing carbon materials, Raman spectroscopy has proven itself to be a versatile tool. It shows accurate and acute detection of the symmetrical vibration of skeleton and functional groups.[31] Meanwhile, as a complement, Fourier transform infrared spectroscopy (FT-IR) shows incredible sensitivity to absorption signals generated from the asymmetrical vibration of functional groups. Combining the merits of both approaches, we are capable of having a clear vision of the product and the reaction. As depicted in Fig. 3c and Fig. S10 (ESI†), three major peaks can be found in the Raman spectra of HsGDY. The D-band located at 1359 cm^{-1} is assigned to the defects/edges, and the G-band at 1603 cm^{-1} is attributed to the vibration of the abundant benzene rings. The peak at 2227 cm^{-1} corresponds to the vibration of alkynyl bonds.[30] The FT-IR spectra of HsGDY in Fig. 3d present four obvious peaks. Among them, the peak at 1579 cm^{-1} is caused by the skeletal vibrations of benzene rings and is parallel to the G-band of the Raman spectrum (Fig. 3c). The stretching and bending vibrations of the C–H bonds of the benzene rings lead to peaks at 2923 cm^{-1} and 875 cm^{-1}, respectively. These three signal peaks demonstrate the existence of aromatic rings in the sample. The peak at 2200 cm^{-1} is assigned to the typical stretching vibration of the alkynyl bond, which is also parallel to the Raman spectrum, indicating the formation of a conjugated diyne linkage.[16,32] We also analyse the Raman and FT-IR spectra of the **tBEP** monomer. An obvious intensity decrease of the peak at 994 cm^{-1} can be observed in the Raman spectrum (Fig. S7, ESI†). As for the FT-IR spectra (Fig. 3d), the intensity of the peak at 617 cm^{-1}, belonging to the stretching vibration of C–Br, significantly decreases after the reaction. Combined with the spectra mentioned, the variations of these two signal peaks indicate the occurrence of the dehalogenative homocoupling reaction and the formation of HsGDYs.

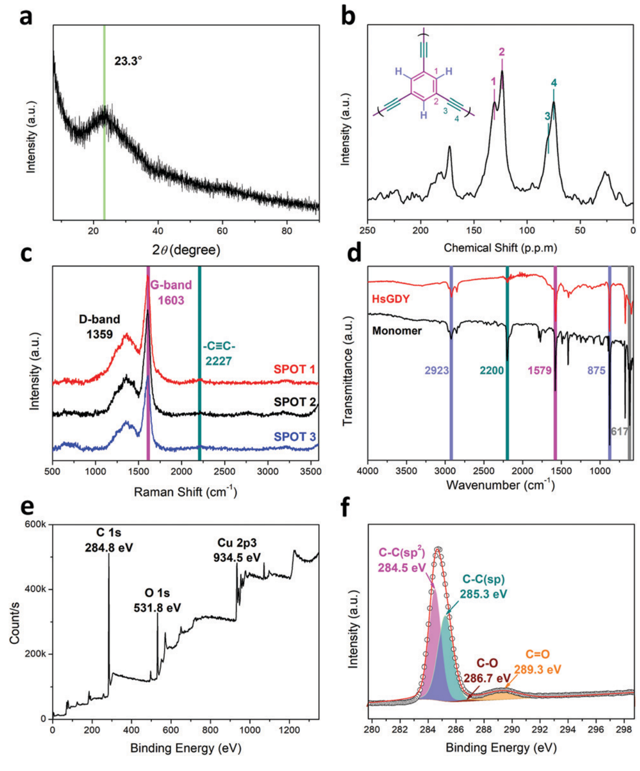

Fig. 3 The structure of HsGDY. (a) XRD patterns of HsGDY. (b) The ^{13}C solid-state NMR spectrum of HsGDY. (c) Raman spectra of three random spots on a HsGDY film. (d) FT-IR spectra of the monomer and HsGDY film. (e and f) XPS total spectrum (e) and high resolution C 1s spectrum (f) of HsGDY.

To identify the hybridization status of carbon, X-ray photoelectron spectroscopy (XPS) was conducted. As shown in Fig. 3e, the as-prepared HsGDY film contains three major elements: C (78.9%), O (14.3%) and Cu (2.73%), among which Cu mainly comes from the copper foil. The C 1s peak can be deconvoluted into four subpeaks: 284.5 eV, 285.3 eV, 286.7 eV and 289.3 eV (Fig. 3f). The peaks at 284.5 eV and 285.3 eV refer to C–C (sp^2) and C–C (sp) respectively and the area ratio of sp^2/sp is nearly 1. This number is consistent with the theoretical structure of HsGDY (Fig. 1a) and demonstrates the successful formation of HsGDYs.[11,12,16] On the other hand, the peaks at 286.7 eV and 289.3 eV refer to C–O and C═O and the O1s peak can be additionally assigned to carbonyl (C═O), ester (O═C–O) and hydroxyl (O–H) (Fig. S8, ESI†).[33,34] The appearance of these bonds indicates that oxygen slightly dopes HsGDY, which may partly alter the localized electronic structures and eventually affect the properties.[34]

Due to the extended π-conjugated system and the macro/mesoporous second-order structure, HsGDY provides a huge number of tunnels and interspaces for ion transmission and storage.[11,12,35] The HER and OER catalytic performances of HsGDYs were investigated with a typical three-electrode system in 1M KOH. The as-prepared HsGDY on copper foil was directly used as the working electrode without further treatment. As depicted in Fig. 4a and b, the overpotential required for HsGDYs to reach a current density (j) of 10 mA cm^{-2} is 531 mV and the Tafel slope is 363 mV dec^{-1}. As for the OER, HsGDY exhibits an overpotential of 646 mV at 10 mA cm^{-2} with a Tafel slope of 128 mV dec^{-1} (Fig. 4c and d). HsGDY we obtained exhibits a similar HER/OER activity to that in previous studies, like exfoliated graphdiyne (690 mV for the HER) and GDY (445 mV for the OER).[7,36] The small number of O-containing functional groups in our sample may somewhat decrease the continuity of the planar π-conjugation system and decrease the charge carrier mobility and electrical conductivity.[37] We suggest that HsGDY can achieve much better catalytic performance when combined with other metal atoms.[7,12,36] In contrast to the stability of graphene, the sp hybridized linkages (–C≡C–) of HsGDYs possess higher reactivity, which can chelate metal atoms more firmly and thus boost the catalytic performance.[5,6,29]

In summary, combining the traditional synthesis strategy of GDY and our previous result of surface chemistry, we utilized a new monomer **tBEP** and successfully prepared the HsGDY film on copper foils *via* the dehalogenative homocoupling reaction.

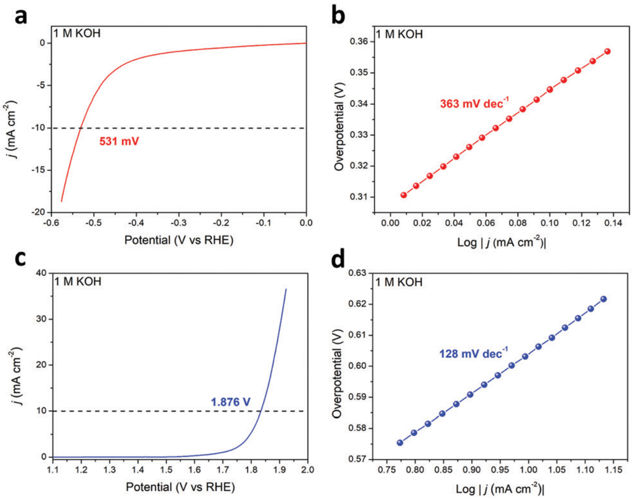

Fig. 4 HER/OER catalytic performance of HsGDY. (a) The polarization curve for the HER. (b) The corresponding Tafel plot. (c) The polarization curve for the OER. (d) The corresponding Tafel plot.

The HsGDY film is a free-standing, carbon-rich material with a meso/macroporous second-order structure. Qualitative and quantitative measurements demonstrate the existence of abundant aromatic rings and alkyne bonds. The ratio of sp^2 to sp carbon atoms is close to 1 : 1, consistent with the theoretical structure of HsGDYs. Compared with previous methods, our reaction can proceed at r.t. without extra heating and the reaction time is also shortened from over 24 h to 12 h. This delightful improvement is mainly attributed to the terminal alkynyl bromide functional groups which have higher stability than alkynyl and higher reactivity than alkynylsilane. The HER and OER catalytic performances were also measured. HsGDY shows a similar electrochemical activity to that in previous studies. This work not only proposes a novel synthesis strategy for HsGDYs, but also provides a potential solution for the large-scale industrial preparation of GDYs.

This study was supported by the National Natural Science Foundation of China (No. 21905206) and the Shanghai Sail Program (No. 19YF1450800).

Conflicts of interest

There are no conflicts to declare.

Notes and references

1 G. Luo, X. Qian, H. Liu, R. Qin, J. Zhou, L. Li, Z. Gao, E. Wang, W.-N. Mei, J. Lu, Y. Li and S. Nagase, *Phys. Rev. B: Condens. Matter Mater. Phys.*, 2011, **84**, 075439.

2 J. Li, S. Li, Q. Liu, C. Yin, L. Tong, C. Chen and J. Zhang, *Small*, 2019, **15**, 1805344.

3 N. Wang, J. He, Z. Tu, Z. Yang, F. Zhao, X. Li, C. Huang, K. Wang, T. Jiu, Y. Yi and Y. Li, *Angew. Chem., Int. Ed.*, 2017, **56**, 10740–10745.

4 Z. Yang, X. Shen, N. Wang, J. He, X. Li, X. Wang, Z. Hou, K. Wang, J. Gao, T. Jiu and C. Huang, *ACS Appl. Mater. Interfaces*, 2019, **11**, 2608–2617.

5 J. Li, J. Xu, Z. Xie, X. Gao, J. Zhou, Y. Xiong, C. Chen, J. Zhang and Z. Liu, *Adv. Mater.*, 2018, **30**, 1800548.

6 Y. Guo, J. Liu, Q. Yang, L. Ma, Y. Zhao, Z. Huang, X. Li, B. Dong, X. Z. Fu and C. Zhi, *Small*, 2020, **16**, 1907341.

7 H. Yu, Y. Xue, L. Hui, F. He, C. Zhang, Y. Liu, Y. Fang, C. Xing, Y. Li, H. Liu and Y. Li, *Nano Energy*, 2019, **64**, 103928.

8 L. Hui, Y. Xue, B. Huang, H. Yu, C. Zhang, D. Zhang, D. Jia, Y. Zhao, Y. Li, H. Liu and Y. Li, *Nat. Commun.*, 2018, **9**, 5309.

9 M. Zhang, X. Wang, H. Sun, N. Wang, J. He, N. Wang, Y. Long, C. Huang and Y. Li, *ACS Cent. Sci.*, 2020, **6**, 950–958.

10 Z. Yang, R. Liu, N. Wang, J. He, K. Wang, X. Li, X. Shen, X. Wang, Q. Lv, M. Zhang, J. Luo, T. Jiu, Z. Hou and C. Huang, *Carbon*, 2018, **137**, 442–450.

11 J. He, N. Wang, Z. Cui, H. Du, L. Fu, C. Huang, Z. Yang, X. Shen, Y. Yi, Z. Tu and Y. Li, *Nat. Commun.*, 2017, **8**, 1172.

12 S. Zhuo, Y. Shi, L. Liu, R. Li, L. Shi, D. H. Anjum, Y. Han and P. Wang, *Nat. Commun.*, 2018, **9**, 3132.

13 S. Debnath, C. Phan, D. J. Searles and M. Hankel, *ACS Appl. Energy Mater.*, 2020, **3**, 7404–7415.

14 Y. Song, X. Li, Z. Yang, J. Wang, C. Liu, C. Xie, H. Wang and C. Huang, *Chem. Commun.*, 2019, **55**, 6571–6574.

15 R. H. Baughman, H. Eckhardt and M. Kertesz, *J. Chem. Phys.*, 1987, **87**, 6687–6699.

16 G. Li, Y. Li, H. Liu, Y. Guo, Y. Li and D. Zhu, *Chem. Commun.*, 2010, **46**, 3256–3258.

17 X. Gao, H. Liu, D. Wang and J. Zhang, *Chem. Soc. Rev.*, 2019, **48**, 908–936.

18 X. Kan, Y. Ban, C. Wu, Q. Pan, H. Liu, J. Song, Z. Zuo, Z. Li and Y. Zhao, *ACS Appl. Mater. Interfaces*, 2018, **10**, 53–58.

19 R. Matsuoka, R. Sakamoto, K. Hoshiko, S. Sasaki, H. Masunaga, K. Nagashio and H. Nishihara, *J. Am. Chem. Soc.*, 2017, **139**, 3145–3152.

20 J. Zhou, X. Gao, R. Liu, Z. Xie, J. Yang, S. Zhang, G. Zhang, H. Liu, Y. Li, J. Zhang and Z. Liu, *J. Am. Chem. Soc.*, 2015, **137**, 7596–7599.

21 J. Li, Z. Xie, Y. Xiong, Z. Li, Q. Huang, S. Zhang, J. Zhou, R. Liu, X. Gao, C. Chen, L. Tong, J. Zhang and Z. Liu, *Adv. Mater.*, 2017, **29**, 1700421.

22 X. Gao, J. Li, R. Du, J. Zhou, M. Y. Huang, R. Liu, J. Li, Z. Xie, L. Z. Wu, Z. Liu and J. Zhang, *Adv. Mater.*, 2017, **29**, 1605308.

23 X. Gao, Y. Zhu, D. Yi, J. Zhou, S. Zhang, C. Yin, F. Ding, S. Zhang, X. Yi, J. Wang, L. Tong, Y. Han, Z. Liu and J. Zhang, *Sci. Adv.*, 2018, **4**, eaat6378.

24 J. Zhou, Z. Xie, R. Liu, X. Gao, J. Li, Y. Xiong, L. Tong, J. Zhang and Z. Liu, *ACS Appl. Mater. Interfaces*, 2019, **11**, 2632–2637.

25 K. Ikegashira, Y. Nishihara, K. Hirabayashi, A. Mori and T. Hiyama, *Chem. Commun.*, 1997, 1039–1040.

26 Z. Zuo, H. Shang, Y. Chen, J. Li, H. Liu, Y. Li and Y. Li, *Chem. Commun.*, 2017, **53**, 8074–8077.

27 R. Liu, X. Gao, J. Zhou, H. Xu, Z. Li, S. Zhang, Z. Xie, J. Zhang and Z. Liu, *Adv. Mater.*, 2017, **29**, 1604665.

28 Q. Sun, L. Cai, H. Ma, C. Yuan and W. Xu, *ACS Nano*, 2016, **10**, 7023–7030.

29 L. Hui, Y. Xue, H. Yu, C. Zhang, B. Huang and Y. Li, *ChemPhysChem*, 2020, **21**, 2145–2149.

30 J. Wang, S. Zhang, J. Zhou, R. Liu, R. Du, H. Xu, Z. Liu, J. Zhang and Z. Liu, *Phys. Chem. Chem. Phys.*, 2014, **16**, 11303–11309.

31 H. Bao, L. Wang, C. Li and J. Luo, *ACS Appl. Mater. Interfaces*, 2019, **11**, 2717–2729.

32 C. Huang, S. Zhang, H. Liu, Y. Li, G. Cui and Y. Li, *Nano Energy*, 2015, **11**, 481–489.

33 S. Wu, G. Wen, R. Schlogl and D. S. Su, *Phys. Chem. Chem. Phys.*, 2015, **17**, 1567–1571.

34 Q. Yang, Y. Guo, J. Gu, N. Li, C. Wang, Z. Liu, X. Li, Z. Huang, S. Wei, S. Xu, L. Song, J. Fan, Z. Chen, J. Qiu and C. Zhi, *Nano Energy*, 2020, **78**, 105283.

35 Y. Xue, J. Li, Z. Xue, Y. Li, H. Liu, D. Li, W. Yang and Y. Li, *ACS Appl. Mater. Interfaces*, 2016, **8**, 31083–31091.

36 C. Hu, H. Liu, Y. Liu, J.-F. Chen, Y. Li and L. Dai, *Nano Energy*, 2019, **63**, 103874.

37 H. Yan, S. Guo, F. Wu, P. Yu, H. Liu, Y. Li and L. Mao, *Angew. Chem., Int. Ed.*, 2018, **57**, 3922–3926.